

## **Physical modeling of impulsive waves generated by rock landslides in curved gorge-type reservoirs**

\*Linfeng Han<sup>1)</sup>, Pingyi Wang<sup>2)</sup>, Meili Wang<sup>3)</sup> and Xiaoling Li<sup>4)</sup>

<sup>1), 2), 3)</sup> *National Engineering Research Center for Inland Waterway Regulation, Chongqing Jiaotong University, Chongqing 400074, China*

<sup>4)</sup> *Chongqing southwest water transport engineering science institute, China*

<sup>1)</sup> [linfengyue@126.com](mailto:linfengyue@126.com)

### **ABSTRACT**

Rockslides are the most dangerous form of mass-wasting because they incorporate a sudden, incredibly fast-paced release of bedrock along a uniform plane of weakness. These uniform weaknesses are key to identifying rock slides because unlike slumps, flows, or falls, the failed material moves in a fairly uniform direction over a layer of solid, pre-existing rock. The sudden, rapid release of material found in rock slides combined with the sheer size and weight of the material that is falling is what gives these events the potential to have devastating effects on human life and infrastructure. Rockslides are a type of landslide caused by rock failure in which a part of the bedding plane of failure passes through intact rock and material collapses en masse and not in individual blocks. The rock landslides in the experiments were treated as a combination of rigid blocks of various scales, and the sizes of rigid blocks were determined by the spacing of cutting surfaces formed along expanded cracks in three directions.

Impulse waves typically occur in open oceans, bays, lakes and reservoirs as the result of landslides, rockfalls, shore instabilities, avalanches or glacier calvings (Heller 2007). They are particularly relevant for the reservoir environment because the slope may well lose its stability during fast water level rise or draw-down. The short propagation distance combined with long-wave behavior within reservoir areas leads to negligible wave attenuation (Heller et al. 2009). Therefore, the impulse waves will remain enormous energy

---

<sup>1)</sup> Ph.D. Student

<sup>2)</sup> Professor

<sup>3), 4)</sup> Engineer

when they reach the shore or dam, which will cause an incidental wave run-up. The wave run-up along a shoreline or a dam can result in a large damage potential for settlement and infrastructure, even a dam overtopping. Historically, the largest impulse wave run-up caused by landslide in reservoirs was observed in Vaiont, North Italy in 1963. A rock flank failure of  $250 \times 10^6 \text{ m}^3$  volume slid into the water body, displacing almost the entire reservoir volume. Wave run-up was observed in villages located 200 m above reservoir level at the opposite shore. The impulse wave also overtopped the arch dam by more than 70 m thereby destroying the village Longarone with more than 2,000 deaths (Schnitter 1964). Examples in the Yangtze Three Gorges Reservoir (TGR), with an estimated total number of about 5386 landslides, also faces the serious situation of impulse waves. On June 12, 1985, the Xintan landslide with the total debris volume of  $20 \times 10^6 \text{ m}^3$  and wave amplitude of 49 m occurred, which consequently caused 10 death and destroyed 64 ships (Hang et al. 2014). A recent event occurred on June 24, 2015, an impulse wave of nearly 6 m in height generated by Hongyanzi landslide with a volume of  $23 \times 10^4 \text{ m}^3$  had overthrew 13 boats, killed 2 persons and injured 4 persons, the maximum wave run-up reached 2 m (Huang et al. 2016).

Hall and Watts (1953) investigated solitary wave run-up with a watertight, linearly inclined slop. They stated that the run-up height depended on the initial relative wave height, offshore still water depth, and beach slope. A breaking criterion for solitary wave run-up was defined by Synolakis (1987) based on an analytical derivation and the experimental data for a gentle slop of 1:19.85(V:H). Comparing with nonbreaking waves, he found the run-up height for breaking waves is significantly smaller. Müller (1995) analytically considered solitary and cnoidal wave run-up and dam overtopping for nonbreaking waves with dam slopes of 1:1, 1:3 and vertical walls. Li and Raichlen (2001) analyzed the solitary wave run-up by nonlinear theory and improved the run-up relation of Synolakis (1987) by introducing a higher-order boundary condition, as a result, approximately 10% higher run-up values resulted with a better agreement to the experimental data. Fuchs and Hager(2012) studied scale effects of impulse wave run-up and run-over with a 2D linearly inclined slop. They found there are no scale effects for solitary wave run-up with still-water depths exceeding 0.08m if the test parameters have a minimum overland flow Reynolds number of 6,300 and a minimum overland flow Weber number of 10. A solitary impulse wave transformation to overland flow was conducted by Fuchs and Hager (2015). From their study result prediction equation specified for the plane wave run-up height at the transition point for a connected horizontal plane.

The landslides that exist in reservoir areas are made up of different materials including rock, soil, debris, or a combination of these. The materials may move by falling, toppling, sliding, spreading, or flowing. The various types of landslides differentiated by the kinds of material involved and the mode of movement will result in different characteristics of impulsive waves (e.g. wave energy, wave amplitude, wave types, wave height). Currently, the slide model studies have been mainly divided into block models and granular models. The studies of Russell (1837) is considered to be the earliest research on landslide generated impulse waves. In his experiments, a box at the end of a wave channel was vertically dropped to produce solitary waves. And since then, many investigators repeated Russell's

experiment to verify mathematical models (Noda 1970; Wiegel et al. 1970), or to investigate the effect of the basic parameters on impulse wave generation (Bukreev and Gusev 1996; Panizzo et al. 2002 & 2005). However, the block models can't reflect the real deformation of slide mass during impact, which leads directly to the experimental results much larger than real values. The difference in block and granular slide model may be attributed to the difference in porosity, slide front angle, blockage ratio, transition at slope toe and slide rigidity (Heller and Kinnear, 2010). As early as the 1970s-80s, Davidson et al. (1974) and Huber (1980) had researched the landslide generated impulse waves using both 2D and 3D granular slide models. In recent years, most studies on impulse waves with granular landslides have focused on the near field characteristics (Fritz 2002; Fritz et al. 2004; Heller 2007; Mohammed et al. 2012 & 2013; Mcfall et al. 2016). Nevertheless, for the granular model the dimension of the blocks were relative small, can't describe the cataclastic structure of rock formation.

Presently, mainly predictive studies focus on the maximum run-up height at the shore opposite to the wave generation, but the run-up variation along reservoir bank have rarely been addressed. In this paper, three major aspects of wave run-up are researched based on rockslide model: (1) the physical modeling of impulse wave generated by rock landslides; (2) the calculation of maximum run-up height and comparison with previous predictions; (3) the run-up variation along reservoir bank. The research results add to the improved risk assessment of landslide hazards in reservoir environment.

## **Physical Model**

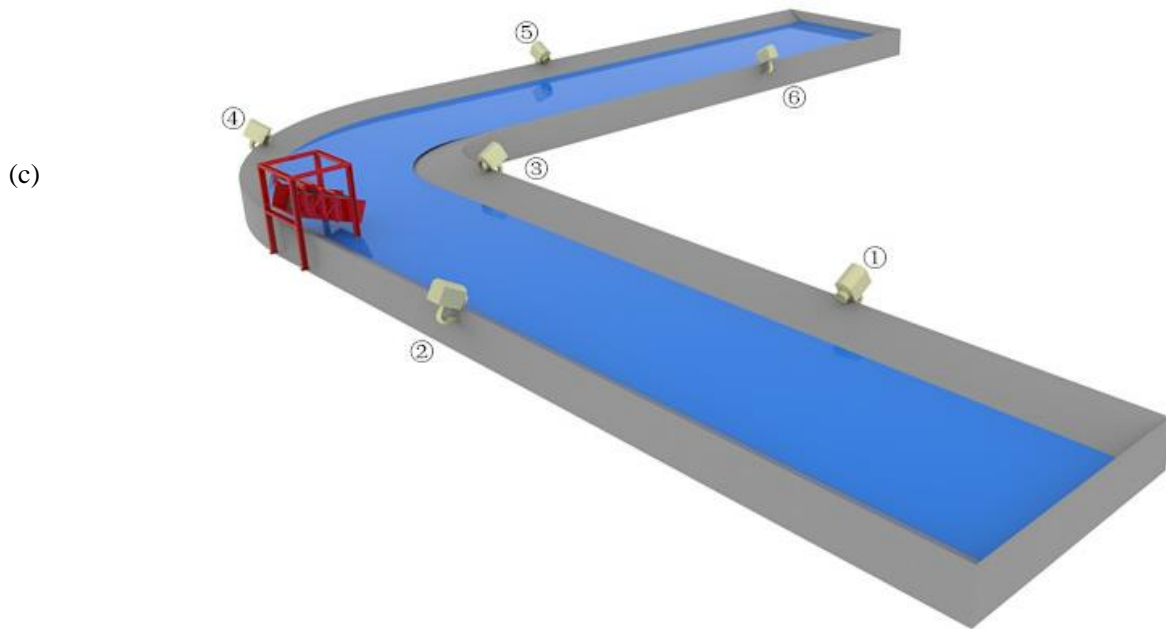
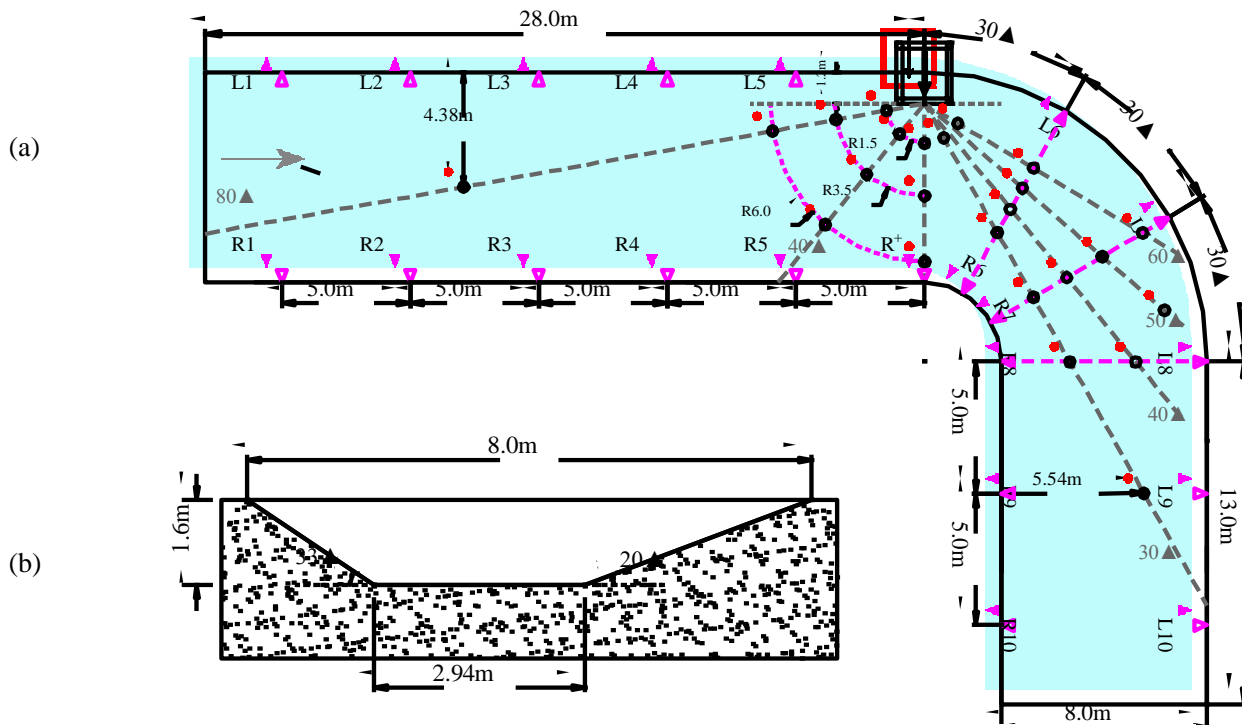
### **Experimental Set-up**

The laboratory experiments on rock landslide generated tsunamis were conducted in the large-scale bend flume of the National Engineering Research Center for Inland Waterway Regulation (NERC-IWR) at Chongqing Jiaotong University in Chongqing, China. The flume has a centerline length of 48m, with a 28m long upstream section, followed by a 90° bend section, with an inner radius  $R_1 = 3\text{m}$  and an outer radius  $R_2 = 11\text{m}$ , and a 13m long downstream section [Fig.1(a)]. The cross-sectional channel of the flume is trapezoid, with a depth of 1.6m, a bottom width of 2.94m, top width of 8.0m, and both side slopes of 33° (left/outside bank ) and 20° (right/inside bank), which approximately equal to the mean slope of the river bank in TGR [Fig.1(b)]. At the entrance of the outside bend a tailored chain-reversing landslide tsunami generator was built into the flume as shown in Fig.1(d), which allowed to simulate landslides with varying volume and hillslope. The generator consists of a sliding box filled up with 1.95m<sup>3</sup> of landslide material whose slope and position are controlled by means of four chain hoists. The iron plates on both sides of the box can be moved optionally to satisfy the requirements of different widths. As the gate opened, the landslide material exits the slide box to accelerate solely by gravity towards the water surface. Landslides were deployed into water depths,  $h$ , of 0.74, 0.88 and 1.16m. The hill slope angle  $\alpha$  was variable from 20° to 60° in the present study.

The following four initial investigated parameters governing the wave generation were varied: still-water depth  $h$ , slide thickness  $s$ , slide width  $w$ , hill slope angle  $\alpha$ . The slide thickness and width determined the slide volume  $V_s$ , and slide volume and hill slope determined the slide impact velocity  $v_s$ . The above four factors with three levels respectively were designed into 81 groups of experiments and their results are shown in Table 1 (end of this paper).

A high-speed camera, with its optical axis perpendicular to the landslide, was deployed to capture temporally resolved details of the landslide kinematics, particularly the landslide front velocity. A total of 24 wave gauges were installed in the bend flume to recorded the wave propagation in radial and angular direction away from the landslide source. The wave gauge configuration in the bend flume at water depth of  $h=0.88\text{m}$  is shown in Fig.1(a). The gauge has a resolution of 1mm and a recording frequency of 100Hz. Twenty-one wave runup measuring points were arranged along the side slopes (No. L1, L2, ...L10, R1, R2, ...R10, R+), which were recorded by pre-arranged scaleplates (1mm resolution) in combination with overhead cameras.

For wave phenomena involving a free water surface, the scale effects would influence transferability of the test data to prototype conditions owing to viscosity or surface tension. According to Fuchs and Hager (2012), the scale effects are insignificant for wave run-up if still-water depths  $h \geq 0.08\text{m}$ . In this experiment, the minimum still-water depth was 0.74m, above which the scale effects can be ignored. Hughes (1993) demonstrated that the effect of surface tension on gravity waves is less than 1% for still water depths  $h \geq 0.02\text{m}$  and wave periods  $T \geq 0.35\text{s}$  for pure water. This test parameters for the primary waves measured at wave source were  $0.74\text{m} \leq h \leq 1.16\text{m}$ , and  $1.16\text{s} \leq T \leq 4.65\text{s}$ . Surface tension effects for pure water are negligible herein, therefore.



(d)

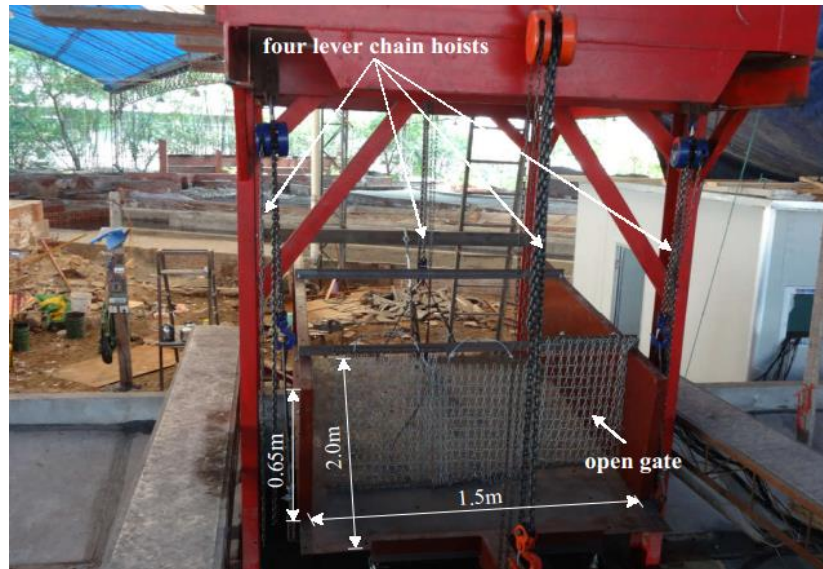


Fig.1 Experimental set up: (a) The wave gauge array used to measure the water surface elevation of the tsunami wavefronts generated by the rock landslides; (b) cross-sectional view (looking downstream) of channel geometry for which depth is 1.6m, side slope angles  $\beta_1=33^\circ$ (outside bank) and  $\beta_2=20^\circ$ (inside bank); (c) Schematic test setup; (d) chain-reversing landslide tsunami generator

## Rock Slide Model

Rock landslide in reservoir area is mainly composed of rock body, all kinds of structural plane (soft stratum, fracture, fault, etc.) and interstice between rock masses. The opening and widening cracks separate fragments of the massif and prepare them for gravitational transport because of stress relaxations occurring along the joints (Margielewski and Urban 2003). These tension cracks are the initial forms preceding the rock movements and become the cutting surfaces during landslide formation[Fig.2(a)]. When the shearing stress exceeds the marginal value, the rock masses will move along the shearing zone and break down into sized chunks during the process of sliding [Fig.2(b)]. In this experiments, rock landslides were treated as a variety scale of rigid blocks by order of triaxial cracks (transverse, longitudinal and vertical), which may be better to reflect the evolution of the rock mass separation by cracks. Table 2 summarizes the crack development of the typical rock landslides in the TGR. The triaxial cracks put together is the size of slide blocks, which decides the dispersion degree of rock mass during the process of sliding. According to the sediment gradation theory, the crack composition curves are fitted out based on the data in Table 2, shown in Fig.3 (the red lines are the curves of model with a scale of 1:70). The characteristic values of the slide blocks selected from the crack composition curves include  $D_{max}$ ,  $D_{60}$ ,  $D_{40}$ ,  $D_{20}$ ,  $D_{10}$ , meanwhile, the combination size of the blocks should meet the overall dimensions of the landslides. Hence, five sizes of slide blocks were produced according to the characteristic values of the composition curves (see Table 3), and the

proportions of blocks for each landslide scheme were shown in Table 4. The rock landslides located in the TGR are composed mainly of mudstone with density  $2.45\text{g/cm}^3$ - $2.65\text{g/cm}^3$  and sandstone with density  $2.2\text{g/cm}^3$ - $2.7\text{g/cm}^3$ . In present tests, the blocks composited of cement and gravels [Fig.4(a)], their density was set to  $2.5\text{g/cm}^3$ . Finally, the rock slide model was created as shown in Fig.4(b).

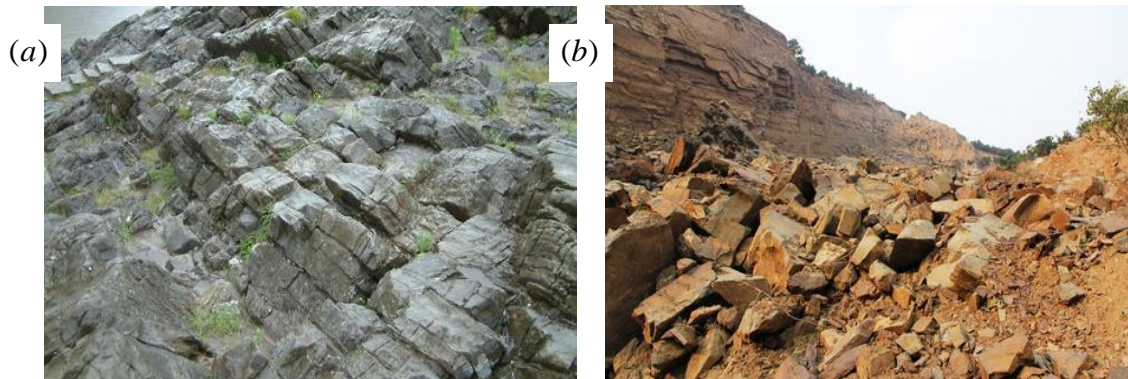
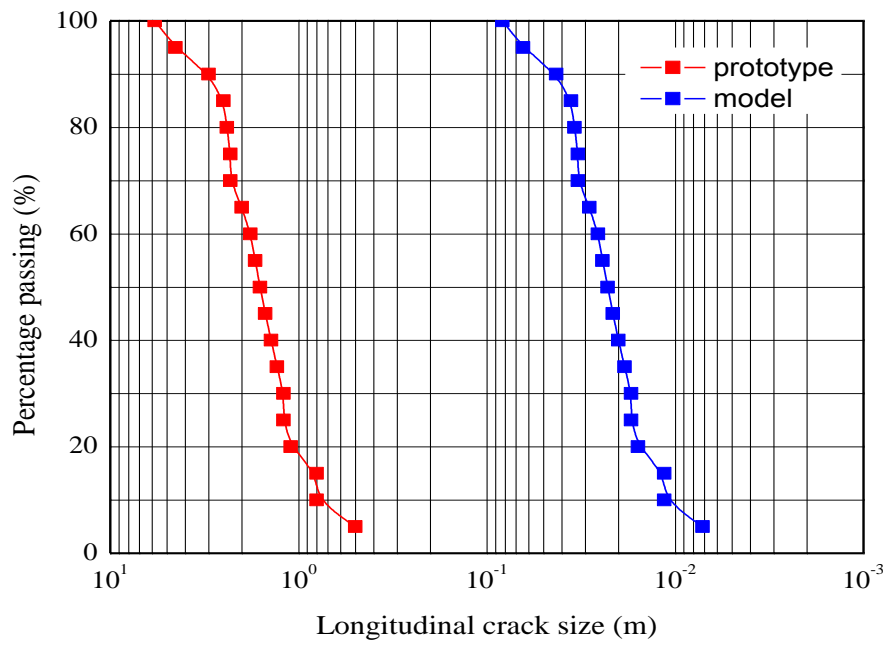
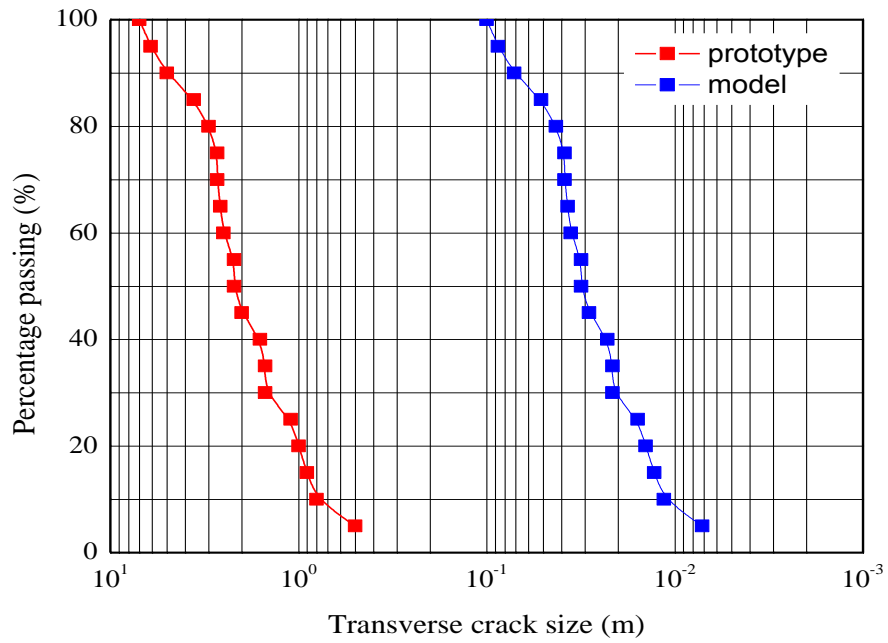


Fig.2 Stages of the rock landslide development in reservoir area: (a) first stage developed as tension cracks and cutting surfaces; (b) succession of landslide developed in effect of the cracks propagation

Table 1 Statistics of crack spacing of typical rock landslides in the TGR

Location	Transverse crack (m)	Longitudinal crack (m)	Vertical crack (m)	Mean crack (m)
Fengjiaba 1# rockslide/ Wushan County	2.2	1.5	0.6	1.4
Wuzhong rockslide/ Fuling County	3.0	3.0	1.2	2.4
Zhanjiawan rockslide/ Fengdu County	1.5	0.8	1.0	1.1
Canlian rockslide/ Wushan County	2.5	2.0	1.5	2.0
Caojiezi rockslide/ Wanzhou County	2.6	1.6	1.6	1.9
Ziyangcheng rockslide/ Fengjie County	1.0	2.3	2.1	1.8
Guling rockslide/ Yunyang County	1.5	2.5	2.2	2.0
Guantangkou rockslide/ Wanzhou County	2.0	1.4	2.4	1.9
Guoyuanchang rockslide/ Wushan County	1.6	1.3	2.9	1.9
Hefengxiang rockslide/ Fengjie County	2.7	1.8	3.3	2.6
Kangjiazui rockslide/ Kaizhou County	7.0	5.8	10.3	7.7
Qukouzhen rockslide/ Kaizhou County	5.0	1.2	3.5	3.2
Shangxiping rockslide/ Wushan County	3.6	2.4	3.7	3.2
Xituo rockslide/ Shizhu County	6.1	4.5	7.4	6.0
Fengjiaba 2# rockslide/ Wushan County	2.2	1.7	3.8	2.5
Banzulin rockslide/ Wanzhou County	0.9	0.8	8.8	3.5
Hualishu rockslide/ Fengjie County	0.5	0.5	3.9	1.6
Erdaogou rockslide/ Wushan County	0.8	1.1	4.1	2.0
Yuhuangge rockslide/ Wushan County	1.1	1.2	4.5	2.2
Tangjiao 2# rockslide/ Wanzhou County	2.7	2.3	5.1	3.3
Mean (m)	2.5	2.0	3.7	2.7



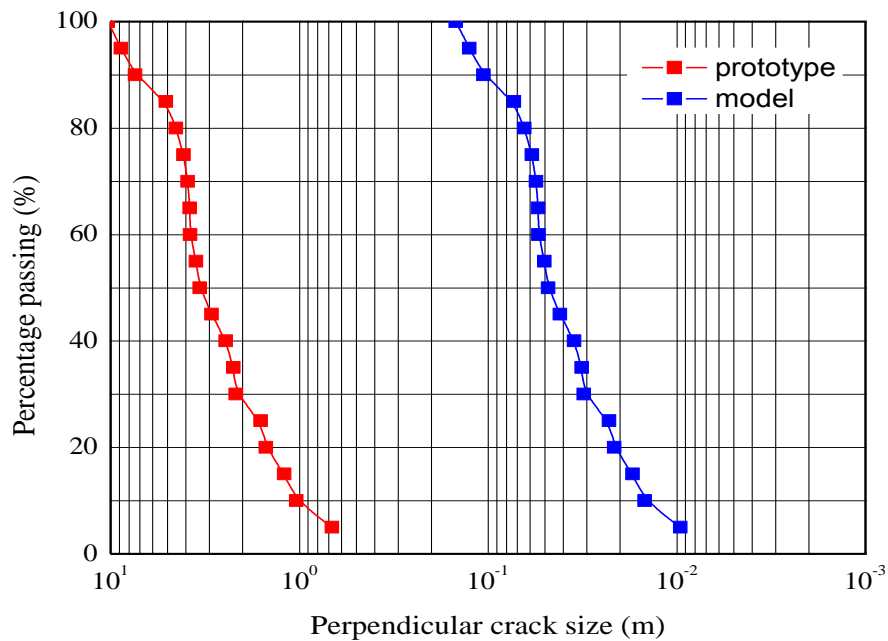


Fig.3 Crack composition curves of rock landslide in TGR

Table 3 Size of slide block

Block no.	Length (cm)	Width (cm)	Thickness (cm)
A1	21	14	6
A2	18	12	5
A3	15	10	4
A4	12	8	3
A5	9	6	2

Table 4 Mix proportions of rigid blocks for rockslide

No.	Number of blocks					Slide size (m) (LxWxT)	Slide volume (m <sup>3</sup> )
	A1	A2	A3	A4	A5		
1	23	19	33	35	93	1.0x0.5x0.2	0.1
2	45	37	67	69	185	1.0x1.0x0.2	0.2
3	45	37	67	69	185	1.0x1.5x0.2	0.3
4	68	56	100	104	278	1.0x0.5x0.4	0.2
5	68	56	100	104	278	1.0x1.0x0.4	0.4
6	91	74	133	139	370	1.0x1.5x0.4	0.6
7	136	111	200	208	556	1.0x0.5x0.6	0.3
8	136	111	200	208	556	1.0x1.0x0.6	0.6
9	204	167	300	313	833	1.0x1.5x0.6	0.9

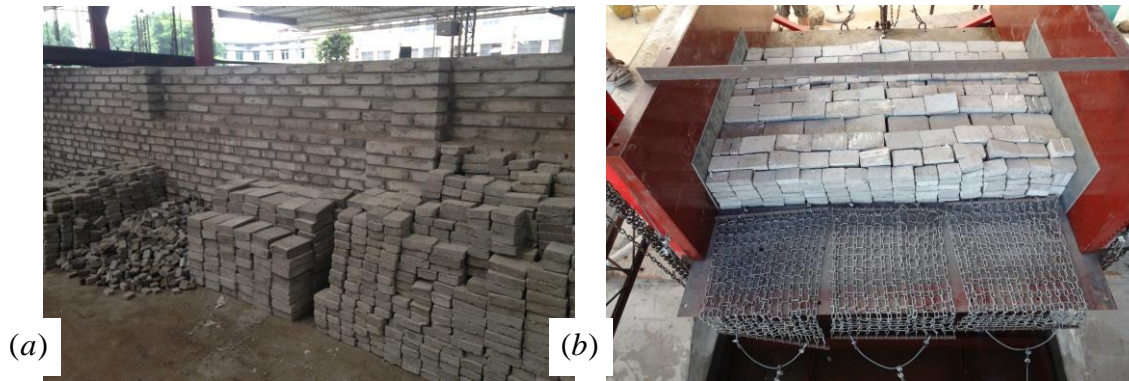


Fig.4 Rock slide model in the experiment test: (a) landslide block composed of cement and gravels; (b) slide mass composed of a variety scale of rigid blocks arranging in triaxial cracks

## Conclusions

Deep expansion of the initial cracks in the massif causes translational-rotational landslides with noncircular sliding surfaces, which are the most common type in the reservoir area. In this study, the rock landslide was treated as a variety scale of rigid blocks by order of the crack developments of rock mass, which reflected the structural nature of the rock landslide better relative to other models. Physical experiments were conducted focusing on wave run-up variation along reservoir bank based on above model. The main results of this experimental study are: The maximum run-up was located in the other side of the wave generation. Compared with previous studies, the maximum run-up predicted by rock slide model was less than the results from other models. According to the topography of river channel, the run-up changing along reservoir bank was divided into four parts: one at the straight section opposite to the wave generation, one at the bend section; a third section was on the straight section at the same bank of the wave generation, and fourth at the bend section. With the increase of propagation distance, the run-up height in Part I, III, IV decreased. But when the observation point was located at sections  $30^\circ$  opposite to the wave generation in Part II, the run-up height almost equal to the maximum, which is one of the important index for reservoir hazard evaluations. Four new equations for computing the run-up changing along bend are developed. Because the present study was conducted in a fixed bank trapezoidal channel, additional work remains to confirm the presented experiments for a alterable channel bank.